World Academy of Science, Engineering and Technology
International Journal of Aerospace and Mechanical Engineering
Vol:8, No:11, 2014

Development of a New Method for T-joint Specimens Testing under Shear Loading

R. Doubrava, R. Růžek

***Abstract*—**Nonstandard tests are necessary for analyses and verification of new developed structural and technological solutions with application of composite materials. One of the most critical primary structural parts of a typical aerospace structure is T-joint. This structural element is loaded mainly in shear, bending, peel and tension. The paper is focused on the shear loading simulations. The aim of the work is to obtain a representative uniform distribution of shear loads along T-joint during the mechanical testing. A new design of T-joint test procedure, numerical simulation and optimization of representative boundary conditions are presented. The different conditions and inaccuracies both in simulations and experiments are discussed. The influence of different parameters on stress and strain distributions is demonstrated on T-joint made of CFRP (carbon fibre reinforced plastic). A special test rig designed by VZLU (Aerospace Research and Test Establishment) for T-shear test procedure is presented.

***Keywords*—**T-joint, shear, composite, mechanical testing, Finite Element analysis, methodology.

I. Introduction

ADVANCED composite materials are widely used for primary structural applications in aerospace industry. New composite material systems with high specific characteristics, compared to traditional laminates, are developed and produced (for instance non-crimp fabric composites, 3D woven composites, braiding composites, tufting, pinning, etc.) [1]–[7]. Together with the composite material development, higher strength characteristics and credibility of joints are required. The typical joints in aerospace applications are lap shear joint, H-joint, T-joint etc.

Structural assembly of primary structural parts of aircraft is currently performed through the mechanical fasteners (rivets, bolts, etc.). Holes are drilled into the cured components. Load transfer through the fastener elements and load distribution depends on local boundary conditions. Considering the cost and weight saving, the adhesive bonding technology is very advanced.

Therefore, a great effort is focused both on the material (composites, adhesives) development and also on development of new joining techniques without application of mechanical elements. These new approaches and the technological development have to be supported by huge experimental testing programs.

The T-joint is one of the most widely used types of joint in aerospace applications. The T-joint is representative, e.g., for skin-rib, and floor-rib (beams) attachments. The T-joints can be loaded by shear, bending, tension/compression and pull. Simulation of real boundary conditions is one of the biggest problems that occur in frame of experimental testing programs. The paper deals with the shear loading of T-joint part. No experimental procedure for this type of test is standardized. The paper documents T-shear test design, FE analysis of T-shear reference specimens with rivets and influence of boundary conditions and other possibly inaccuracies including manufacturing defects on the experimental results. A new test procedure, test rig and methodology for T-joint verification under shear loading were designed by VZLU. The paper documents research work carried out during the Cost Effective Reinforcement of Fastener Areas in Composites (CERFAC) project [8].

R. Doubrava and R. Růžek are with the Aerospace Research and Test Establishment (VZLU), Strength of Structures Department, Beranových 130, Praha, Czech Republic (phone: +420-225 115 134; fax: 420-283920018; e-mail: doubrava@vzlu.cz).

II. T-joint Test Design

The main aim of the T-joint tests is verification of design values. Therefore, the test rig has to take into account not only loading requirements but also the representative boundary conditions which conform the real service conditions (stiffness, load distribution, etc.). The paper is focused on the T-joint test under shear stress conditions. For this purpose, a new test rig and test procedure was designed. The design was focused both on achieving of high stiffness of test rig and keeping of uniform distribution of shear stresses along the T-joint specimen during loading up to its failure. The design is based on application of special dovetail guidance. The main objective of its utilization is elimination of any additional displacement in directions which can cause undesirable stresses in the T-joint. Fig. 1 shows a scheme of the designed test rig.

Extensive numerical analyses and simulations of different boundary conditions were performed with the aim of optimization of test conditions and interactions between the test rig and the T-joint specimen. The aim of work was to optimize load distribution and eliminate early failure outside of the critical investigated area of the joint.

Boundary conditions were analyzed considering a wide range of parameters, namely:

- contact between the specimen and the test rig,
- influence of the transition zone geometry of the specimen on the critical failure load and failure location,
- influence of filler stiffness of the T-joints on the structural stiffness and strength reduction.

The paper shows the main results and conclusions based on performed numerical simulations. The analyzed results were

applied on the final test rig and the T-joint test specimen design.

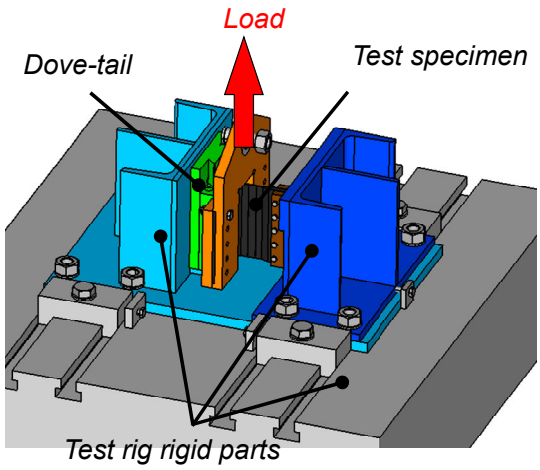

Fig. 1 Schema of the new T-shear test set up

III. T-Joint Composite Sample Model Description

Finite element (FE) models were generated using the FEMAP pre-processor [9]. The commercial FE code NASTRAN [10] was used for FE calculations. Models were made of different types of elements. 2D elements of shell type were used for composite lamina simulation [11]. The properties of lamina layers were defined by the PCOMP property parameter of NASTRAN [10]. The material properties of a lamina are shown in Table I. In Table 1 the E denotes Young's modulus, G = shear modulus and ν = Poisson's ratio.

TABLE I
Mechanical Properties of Composite Material

Material constant	Unit	Value
E_{11}	MPa	65 000
E_{22}	MPa	65 000
G_{12}	MPa	4 900
ν_{12}	-	0.05

The FE model was prepared by discretization of a 3D CAD model of the T-joint specimen. Fig. 2 shows 2D geometry of the T-joint specimen that was modified in order to apply 2D shell type laminate elements. The solid splice plates (tabs) were symmetrically added to the web in the area of specimen connection to the test rig (see Fig. 2 (b)). The aim of tabs was to ensure the identical boundary conditions and correct stress distribution between test rig and test specimen – no significant stress concentrations are acceptable.

Different thicknesses of laminas representative for a typical T-joint part were used in model. The thickness varies from 0.8 mm to 4.9 mm. The web part of the specimen is joined together with the skin through the flange. The flange is joined to the web and to the skin using seven rivets (in one row) with the diameter of 8 mm. Figs. 3 and 4 show the application scheme of the FE mesh in the FEMAP pre-processor with visualisation of a shell lamina thickness. The element side length varies from 1 mm in the rivet holes area to 3 mm in the outer part of the specimen. A global coordinate system was used for material orientation system definition. Orientation of each layer was defined according to this coordinate system by the PCOMP property parameter of the NASTRAN code (see Fig. 3).

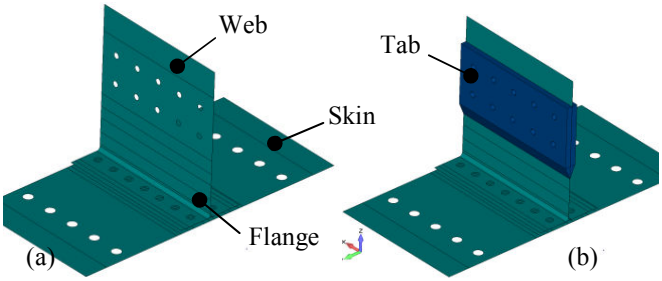

Fig. 2 Modified 2D geometry of T-joint test specimen for shear test (a) and location definition of tabs on the web (b)

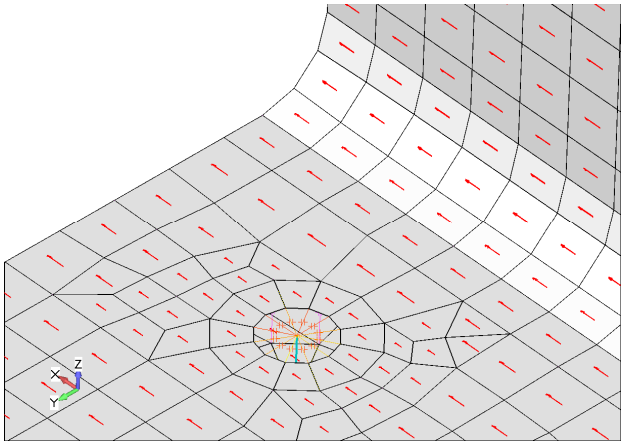

Fig. 3 Material coordinate system in shell elements

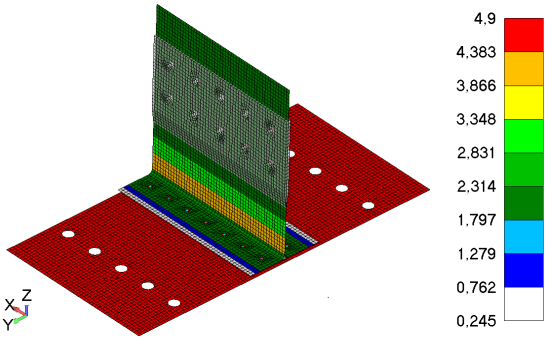

Fig. 4 Contour map of used composite thicknesses (in mm)

1D BEAM elements with mechanical properties of titanium alloys (isotropic material $E = 113$ GPa, $\nu = 0.33$) were used for modelling of mechanical joints (bolts). Two rows of bolts, in each row five bolts with diameter of 8 mm were used for the web part connection of the T-joint specimen to the test rig attachment. The GAP contact elements with characteristics listed in Fig. 5 were used for simulation of the load transfer between fastener dummy shanks and holes.

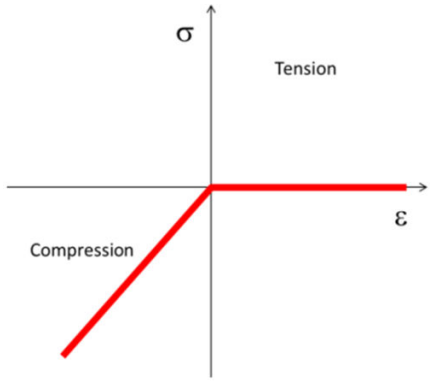

Fig. 5 Property of GAP elements for contact simulation

Fig. 6 shows the schema of FE fastener simulation using combination of multipoint constraint (MPC) for simulation of fastener head, GAP elements for contact simulation and BEAM elements for simulation of axial and bending stiffness of the fastener.

The mesh consists of approximately 16,500 elements.

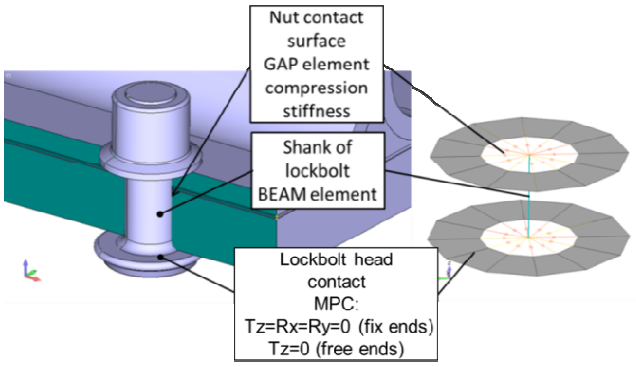

Fig. 6 Description of rivet discretization by FE elements

IV. Analysis of Boundary Condition Influence

The combination of rigid and contact elements was used for simulation of real boundary conditions of the rig for shear load test.

Fig. 7 shows boundary condition definition using coloured areas of surface for shear test simulation. The blue colour defines surfaces with displacement constraint in Z-axis direction for simulation of gripping between steel parts of jig. The yellow colour defines surfaces with fixed constraint. The red colour defines surfaces which have possibility to contact constrain between T-joint specimen and the test rig.

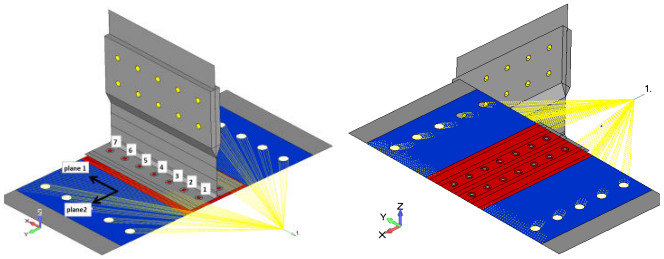

Fig. 7 Boundary condition for shear test simulation

Three different boundary conditions are presented between the test rig and the test specimen surface in the area below the flanges and the web parts (contact, free and fix) – see red colored area in Fig. 7). GAP elements with compression stiffness properties of steel material ($E = 210$ GPa) were used for simulation of contact between the specimen and the test rig. Definition of GAP elements property was the same as it was used for the rivet simulation (Fig. 6).

Unit load of 1 N in X-axis direction for shear loading simulation was used (see Fig. 7). The load was applied using multi-point constraints (MPC). MPC's were created inside of the holes for bolts that attach T-joint specimen to the test rig and at the edge of the skin in the contact area between T-joint specimen and the test rig. The distribution of shear forces to the individual flange rivets evaluated using FE simulation considering different boundary conditions between T-joint test specimen and the test rig is shown in Fig. 8. Three above mentioned different boundary conditions were taken into account: without support of surface in the area below the flanges and the web parts), with contact support of surface in the area below the flanges and the web parts and with fix support of surface in the area below the flanges and the web parts. Individual boundary conditions are denoted in Fig. 8 as without support below the flanges and web, with support below the flanges and web and fix support below the flanges and web. Comparison of different boundary conditions influence on the force transfer through the individual rivets shows the significant influence of considered contact cases, namely for the last No. 7 rivet (lock bolt) – bottom rivet from the load introduction point. Fig. 9 shows the contour map of contact elements displacements between the test specimen and the test rig. Displacements contour map corresponds to unit shear loading case. The force values corresponding to unit shear load were additionally transferred for each individual rivet to the maximum design load. It was supposed the maximum bearing load of 3 000 N for these analyses.

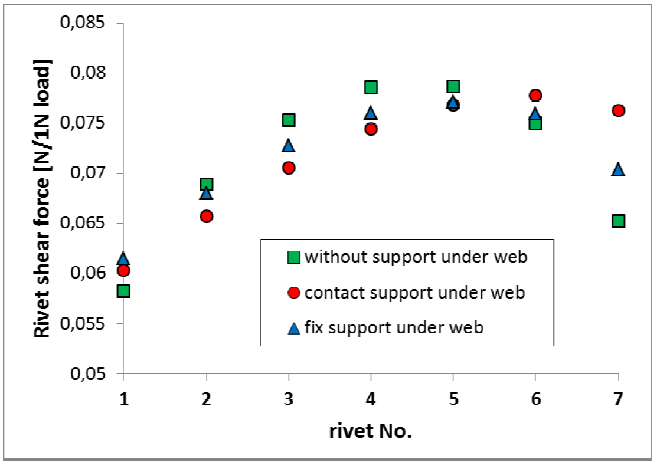

Fig. 8 The influence of different boundary condition between the test specimen and the test rig (in the area below the flanges and the web) on the rivet load distribution

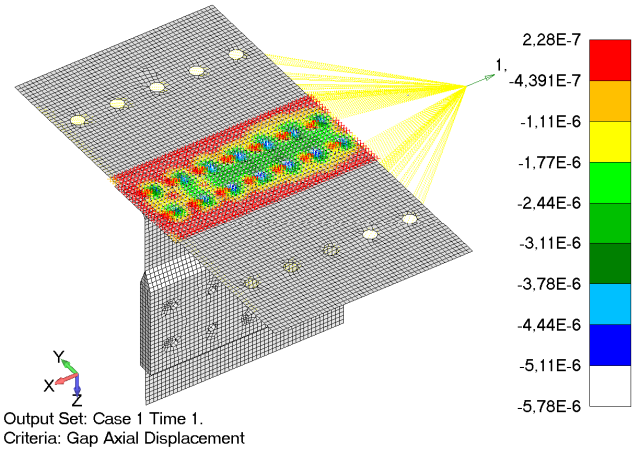

Fig. 9 Contour map of contact displacements in X-axis of the test specimen under unit shear loading (in mm)

Further analysis was focused on the elimination of a specimen thin web overload in the vicinity of the transition area between the test specimen and the test rig. The web of the test specimen is strengthened in this area by tabs. The tabs have variable geometry in the transition area. Three types of ramp geometry of tabs were analyzed: The aim of the work was to decrease strain peaks occurring in the critical transition area. Fig. 10 shows transition area geometry influence on the major strains. The main scope of this optimization process was to decrease the strain peak values in the critical area. Three different ramp geometries were considered – see Fig. 10. The ramp geometry had significant influence on the strain peak occurrence. Fig. 11 shows photographs of the real web fracture in the transition area due to unacceptable strain peak presence.

The previously mentioned analyses of boundary conditions were performed with the aim to define a filler stiffness influence on the mechanical properties of the T-joint. The filler is placed into a deltoid area between a flange and a web of the joint. Example of a real filler placement into the T-joint with obvious manufacturing imperfections is shown in Fig. 12.

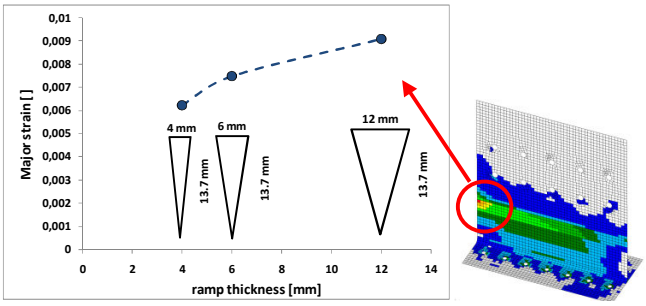

Fig. 10 Optimization of ramp geometry for elimination of failure in the transition area between the web part of a specimen and the rig

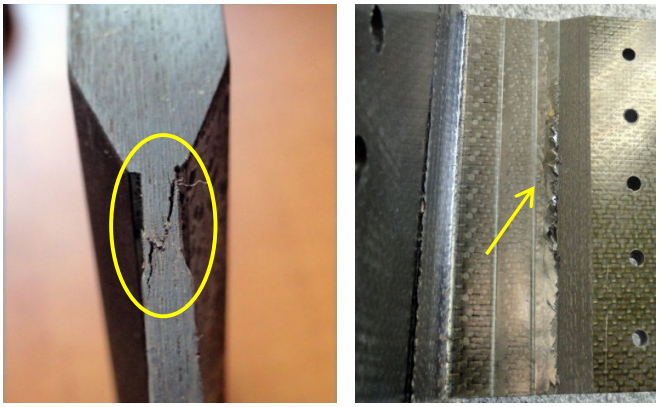

Fig. 11 Examples of improper failure in the web transition area

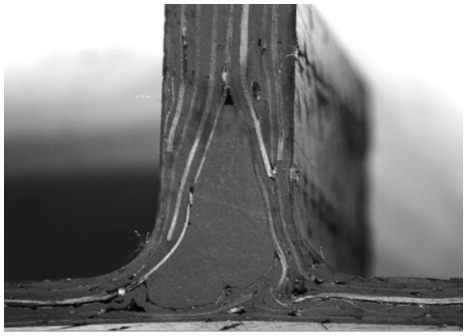

Fig. 12 Example of the T-joint with filler and obvious manufacturing imperfections

The stiffness of this area depends on manufacturing technology. The stiffness is influenced by the filler material, resin, fiber content and fabric and also by the imperfections. Therefore, the analyses included two very different properties of the filler. The proposed FE model of the filler for simulation is illustrated in Fig. 13. Both high stiffness representative for carbon reinforced composite material (CFRP, E = 65 GPa) and low stiffness representative for a foam (E = 1 GPa) was used for the filler area simulations. The solid elements with isotropic material properties were used for evaluation of the filler stiffness influence on the interaction between the test specimen and the test rig.

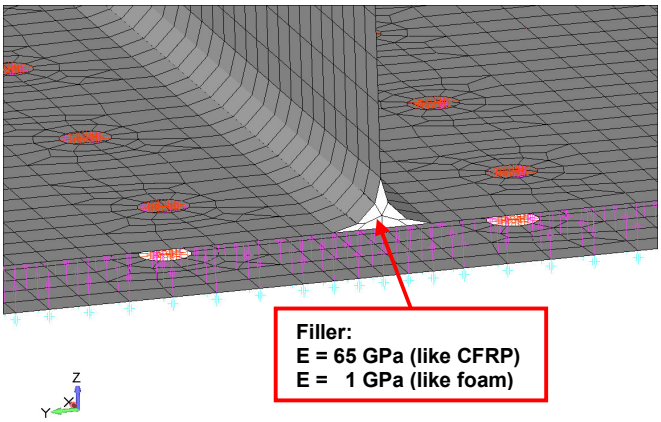

Fig. 13 Proposed FE model for evaluation of the influence of filler stiffness (two different values of filler stiffness)

Fig. 14 shows the filler stiffness influence on the strain distribution in the test specimen and contact forces in the area of contact between the web and skin parts of the T-joint specimen. The strain values correspond to the above defined maximum bearing load level.

Based on the filler stiffness analyses, it can be stated that the high value of filler stiffness (corresponds to CFRP material) gives more uniform shear load distribution (see Fig. 14 (a)) along the middle (web and skin parts contact area) part of T-joint.

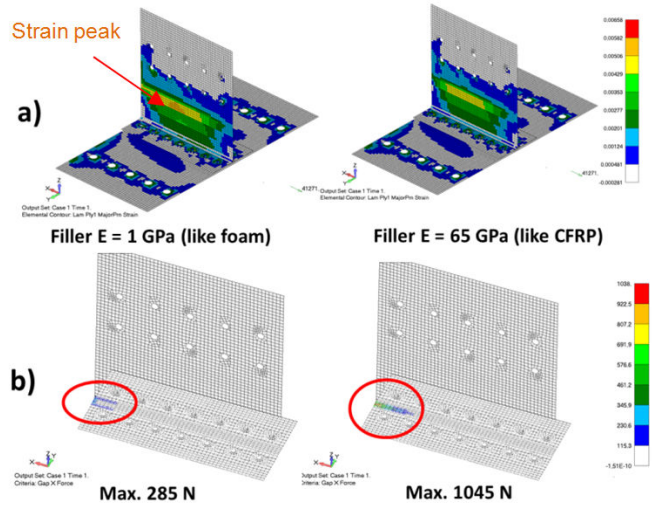

Fig. 14 The influence of the filler stiffness on major principal strain distribution (a) and filler stiffness influence on contact forces in the web and skin parts contact areas of the T-joint specimen (b)

The results also show the influence of filler stiffness on the load transfer through the individual bots in the web transition area (the web part area with tabs attached to the rig) – see Fig. 15. These values are important for optimization of bolts dimensions before manufacturing of T-joint specimens and the test rig. This step is very important in terms of costs saving.

The results based on the filler stiffness analysis show possible overload of a boundary bolt (No. 10) by about 24% in case of low stiffness of filler from a foam material. This parameter is important in terms of damage initialization and strength level of T-joints obtained by experiments.

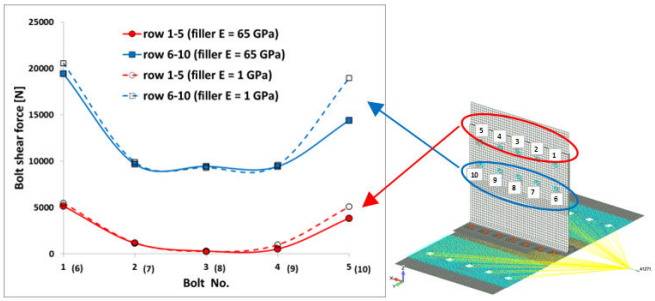

Fig. 15 Filler stiffness influence on loads transferred through the individual bolts in the web transition area between the test specimen and the test rig

V. Conclusion

A new non-standardized procedure of the T-joint test under shear loading is presented. The influence of different boundary conditions on the stress strain distributions in the test specimen and potentially failure modes is discussed. The essential influence of material parameters, geometry of transition area between the test specimen and the test rig, filler parameters and manufacturing imperfections on the failure location and stress and strain distribution was illustrated. The weak point of present day analyses seems to be absence of filler mechanical properties. The web filler stiffness significantly affects the distribution of contact forces and fasteners load distribution.

Acknowledgment

The research leading to these results has received funding from the European Community's Seventh Framework Programme (FP7 – Transport - Cost Effective Reinforcement of Fastener Areas in Composites) under grant agreement n° 266026.

References

[1] C. E. Bakis et al, Fiber-Reinforced Polymer Composites for Construction — State-of-the-Art Review. *J. Compos. Constr.*, 6(2), 2002, 73–87.

[2] F. Weyrauch, L. Llopart, F. Strachauer, An Innovative Approach on Modular Joints for Carbon Fibre Reinforced Structures. *Proceedings of ICCM-17 17th International Conference on Composite Materials*, 27 – 31 Jul 2009, Edinburgh, UK, ISSN, 1465-8011.

[3] K.I. Tserpes, G.N. Labeas, Mesomechanical analysis of non-crimp fabric composite structural parts. *Composite Structures*. 87(4), 2009, 358–369.

[4] F. Stig, S. Hallström, Assessment of the mechanical properties of a new 3D woven fibre composite material. *Composites Science and Technology*, 69(11–12), 2009, 1686–1692.

[5] G. Wachinger, C. Thum, L. Llopart, A. Maier, H. Wehlan, T. Stöven, New Trends in CFRP Treatment and Surface Monitoring for Automated Structural Adhesive Bonding. *Proceedings of ICCM-17 17th International Conference on Composite Materials*, 27 – 31 Jul 2009, Edinburgh, UK, ISSN, 1465-8011.

[6] K.I. Tserpes, , Sp. Pantelakis, V. Kappatos, The effect of imperfect bonding on the pull-out behavior of non-crimp fabric Pi-shaped joints. *Computational Materials Science*. 50(4), 2011, 1372–1380.

[7] D.R. Cartié, G. Dell'Anno, E. Poulin, I. K. Partridge, 3D reinforcement of stiffener-to-skin T-joints by Z-pinning and tufting. *Eng. Fracture Mechanics*, 73(16), 2006, 2532–2540.

[8] CERFAC - Cost Effective Reinforcement of Fastener Areas in Composites. FP7 grant agreement n° 266026, http://research.cenaero.be/~cerfac.

[9] Femap - Finite Element Modeling And Postprocesing, Version 11.1.2. Siemens Product Lifecycle Management Software Inc. 2014.

[10] Nastran - NASA STRucture ANalysis. Finite element analysis code. Version NX/Nastran 8.5. Siemens Product Lifecycle Management Software Inc. 2013.

[11] M. Asif, Y. Aymat, M. Kashif, Design and Analysis of Grid Stiffened Composite structure, Lambert Academic Publishing AG&Co.Kg, Saarbrucken, 2010, ISBN: 978-3-8383-51-1.